Acta Mechanica 191, 195–217 (2007)
DOI 10.1007/s00707-007-0454-8
Printed in The Netherlands

Acta Mechanica

Newtonian flow with nonlinear Navier boundary condition

M. T. Matthews and **J. M. Hill**, Wollongong, New South Wales

Received March 14, 2006; revised January 8, 2007
Published online: May 9, 2007

Summary. The generalized nonlinear Navier boundary condition advocated by Thompson and Troian in the journal *Nature*, and motivated from molecular dynamical simulations, is applied to the conventional continuum mechanical description of fluid flow for three simple pressure-driven flows through a pipe, a channel and an annulus, with a view to examining possible non-uniqueness arising from the nonlinear nature of the boundary condition. For the pipe and the channel it is shown that the results with the nonlinear Navier boundary condition may be obtained from a pseudo linear Navier boundary condition but with a modified slip length. For the annulus, two sets of physically acceptable solutions are obtained corresponding to the chosen sign of the normal derivative of the velocity at each solid boundary. Closer examination reveals that although the generalized Navier boundary condition is highly nonlinear, in terms of the assumed form of solution the integration constants obtained are still unique for the three simple pressure-driven flows presented here, provided that care is taken in its application and noting that the multiplicity of solutions obtained for the annulus arise as a consequence of adopting different signs for the normal derivatives of velocity at the boundaries.

1 Introduction

One of the major themes in science and technology during the past half century has been miniaturization down to the micro and nano scale. The area of micro and nanofluidics is fundamentally important due to the necessity of understanding the nature of fluid flow at this scale [1]. Micro and nanofluidics may be broadly interpreted as the study of mass and momentum transfer, heat transfer, and reactive processes coupled with transport in micro or nano scale systems or around micro or nano sized objects. The first question that must be answered is, 'What happens when a liquid film thickness is comparable to the size of the molecules themselves?' It has been demonstrated that the mechanical properties cannot be understood by extrapolating known properties of the bulk fluid [2]–[4]. One of the main reasons for this is that when devices are scaled down, the surface-to-volume ratio increases dramatically so that surface-related phenomena become increasingly dominant. Hence some qualitatively new features emerge when mechanical structures become sufficiently small, and it becomes important to understand the various types of interactions in the flow and the underlying physical mechanisms, such as the interaction between the constituents of the flow and their interaction with solid boundaries. These interactions are not well understood and are the subject of current fundamental research.

An example of the breakdown of conventional macroscopic ideas at small scales is the no-slip boundary condition between a fluid and a solid, which is a fundamental notion in fluid mechanics [5]–[7]. However, the boundary condition of how momentum is transferred during flow can vary from stick (that is, no slip) to slip, which saves energy in response to physical chemical properties of the solid surface [3], [8]–[14]. Without sufficient knowledge of these phenomena, one cannot systematically design nanofluidic devices or control their operation.

The traditional Navier-Stokes model of fluid flow with a no-slip boundary condition at a fluid-solid interface demands two conditions for its validity [15]:

(i) the fluid is a continuum, which is always satisfied since there are more than one million molecules in the smallest volume in which appreciable macroscopic changes take place;
(ii) the flow is near thermodynamic equilibrium, which is satisfied if there is a sufficient number of molecular encounters during a time period small compared to the smallest time-scale for flow changes. During this time period a molecule would have moved a distance small compared to the smallest flow length scale.

Traditionally the no-slip condition at a fluid-solid interface is enforced in the momentum conservation equations. In other words, the fluid velocity is zero relative to a solid boundary. However, this boundary condition is only valid if condition (ii) given above is satisfied, that is the fluid flow adjacent to the solid surface is in thermodynamic equilibrium. For this to be true, an infinitely high frequency of collisions between the fluid and the solid surface is required. For fluid flow in small scale systems the collision frequency is not high enough to ensure thermodynamic equilibrium, thus a certain degree of tangential velocity slip must be allowed.

Of course, there are many problems at the macro scale where the no-slip boundary condition is clearly inapplicable. The moving contact line where a liquid spreads on a solid surface is a classical example of when a slip flow must be allowed to avoid singular/unrealistic behavior in the Navier-Stokes solutions [16]–[19]. Other examples where slip flow must be allowed include corner flows [20]–[22] and the extrusion of polymer melts from capillary tubes [23]. These and many other paradoxes in fluid mechanics may possibly be an artefact of the no-slip boundary condition, and some fundamentally important paradoxes are reviewed thoroughly in [24].

The nature of boundary conditions in fluid mechanics was widely debated in the 19th century by many of the great names including Bernoulli, Euler, Coulomb, Darcy, Navier, Helmholtz, Poisson, Poiseuille, Stokes, Hagen, Couette, Maxwell, Prandtl and Taylor. Navier [25] introduced the linear boundary condition, later proposed independently by Maxwell [26], which remains the standard characterization of slip used today; namely the component of the fluid velocity tangential to the surface is assumed proportional to the tangential stress, and the constant of proportionality is called the slip length [27]. There have been many attempts to extend this boundary condition to more general flows; in particular it has been extended to include the effects of multiple phases [28]–[34].

Molecular dynamical simulations have also done their part in casting doubt on the applicability of the no-slip boundary condition. Molecular dynamical simulations recognize that a fluid is made up of discrete particles; namely molecules, atoms, ions and electrons, and the position, velocity and state of all the particles at all times are tracked using the laws of classical mechanics. Thompson and Troian [35] provide molecular dynamical simulations to quantify the slip-flow boundary condition dependence on the shear rate. The aim of their simulations was to determine the degree of slip at a solid-liquid interface as the interfacial parameters and the shear rate are varied. At low shear rate the slip length behavior is consistent with the Navier model, but at high shear rates the Navier condition breaks down as the slip length increases rapidly with the

shear rate. Their proposed boundary condition is thus highly nonlinear, even though the fluid is still considered to be Newtonian. That is, the slip length becomes nonlinear and becomes singular at a critical value of the shear rate, well below the shear rate at which the linear stress relation fails, and this deviation from linearity is not gradual, but singular. Based on these results Thompson and Troian [35] proposed a universal boundary condition at a solid-liquid interface.

In this paper the universal nonlinear boundary condition proposed by Thompson and Troian [35] from their molecular dynamical simulations is applied to the continuum mechanical formulation of Newtonian fluid mechanics for three simple pressure-driven flows – in a pipe, between infinite parallel plates and through an annulus. In general the replacement of a simple linear boundary condition (that is, the no-slip boundary condition) by a highly nonlinear one in a continuum mechanical formulation might result in non-uniqueness and interesting behavior, such as multiple solutions which are both mathematically and physically acceptable. The aim of the present analysis is to investigate the effects of the highly nonlinear boundary condition on the well-known solutions of three simple pressure-driven flows. In the following Section the nonlinear Navier boundary condition is described. In the subsequent Sections the pressure-driven flow through a pipe, a channel and an annulus are analyzed for both the linear and nonlinear Navier boundary conditions. Finally, we present a discussion of the results and concluding remarks.

2 The nonlinear Navier boundary condition

The standard no-slip boundary condition is replaced by the nonlinear Navier boundary condition, where the slip velocity is assumed to be proportional to the tangential viscous stress and the degree of slip is measured by a non-constant slip length. For an incompressible Newtonian fluid the viscous portion of the stress tensor or the extra stress is given by $\mathbf{S} = 2\mu\mathbf{D}$, where μ is the viscosity, and the rate of deformation tensor is

$$\mathbf{D} = \frac{1}{2}\left[\nabla\mathbf{v}^* + (\nabla\mathbf{v}^*)^T\right], \tag{2.1}$$

i.e. $\mathbf{S} \propto \mathbf{D}$. At a solid surface the tangential component of velocity is assumed to satisfy the Navier boundary condition [25], [26],

$$v_\parallel = 2\ell^* D_\parallel, \tag{2.2}$$

where ℓ^* is the slip length with the same sign as $D_\parallel$, since in this study it is always assumed that the tangential component of velocity $v_\parallel$ is positive in the direction of flow. Note that at the surface the normal component of velocity is $v_\perp = 0$, and hence all of its derivatives are zero (see [36]), so that $D_\parallel$ will only involve $v_\parallel$ and its derivatives. For the nonlinear Navier boundary condition it is assumed that the slip length ℓ^* depends on the tangential viscous stress at the solid surface via the following relation [35]:

$$\ell^* = \alpha^*\left(1 - 2\beta^* D_\parallel\right)^{-\frac{1}{2}}, \tag{2.3}$$

where

$$\beta^* = \left[2D_{\parallel\text{critical}}\right]^{-1} \tag{2.4}$$

is some critical (maximum) shear rate with the same sign as $D_\parallel$ and the value is such that the inverse square root does not become negative. Note that when $\beta^* = 0$ we have $\ell^* = \alpha^*$, that is α^* corresponds to the constant slip length of the Navier boundary condition.

3 Flow through an infinite pipe

Consider the steady flow of an incompressible Newtonian fluid through an infinite pipe with radius R. The flow is driven by a pressure difference $P_0 - P_L$ acting over a distance L parallel to the pipe. A cylindrical coordinate system (r^*, θ, z^*) will be used, where r^* is measured in the radial direction and z^* is measured in the axial direction positive in the direction of flow. A velocity distribution of the form

$$v_r^* = 0, \quad v_\theta^* = 0, \quad v_z^* = v_z^*(r) \tag{3.1}$$

is assumed such that the mass conservation equation is automatically satisfied and the momentum conservation equation is given by (see [7])

z-component:

$$0 = -\frac{\partial P^*}{\partial z^*} + \frac{\mu}{r^*}\frac{d}{dr^*}\left(r^*\frac{dv_r^*}{dr^*}\right), \tag{3.2}$$

while the r^* and θ^* components yield $\partial P^*/\partial r^* = 0 = \partial P^*/\partial \theta^*$; thus the z^* component may be written

$$\frac{dP^*}{dz^*} = \frac{\mu}{r^*}\frac{d}{dr^*}\left(r^*\frac{dv_r^*}{dr^*}\right). \tag{3.3}$$

Since the left hand side of the above equation is a function of z^* only and the right hand side is a function of r^* only, we have

$$\frac{dP^*}{dz^*} = -A = \frac{\mu}{r^*}\frac{d}{dr^*}\left(r^*\frac{dv_r^*}{dr^*}\right), \tag{3.4}$$

where A is a constant. By applying the boundary conditions $P^* = P_0$ at $z^* = 0$ and $P^* = P_L$ at $z^* = L$, we find that

$$P^* = -Az^* + P_0, \quad A = \frac{P_0 - P_L}{L} > 0, \tag{3.5}$$

hence

$$v_z^*(r^*) = -\frac{A}{4\mu}r^{*2} + C_1^* + C_2^* \ln r^*, \tag{3.6}$$

where C_1^* and C_2^* are integration constants to be found. For the solution to be bounded at the centerline of the pipe it is required that $C_2^* = 0$. By introducing the dimensionless variables

$$v_z = \frac{4\mu v_z^*}{AR^2}, \quad r = \frac{r^*}{R}, \tag{3.7}$$

we have simply

$$v_z(r) = -r^2 + C_1. \tag{3.8}$$

Note that

$$\left.\frac{dv_z}{dr}\right|_{r=1} = -2. \tag{3.9}$$

With a no-slip boundary condition at the inner surface of the pipe we have $v_z = 0$ when $r = 1$ so that Eq. (3.8) becomes

$$v_z(r) = 1 - r^2, \tag{3.10}$$

which is the standard parabolic profile shown in Fig. 1.

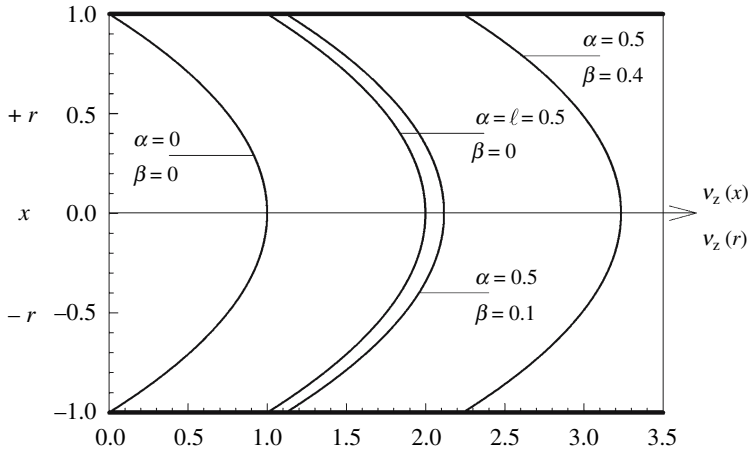

Fig. 1. Velocity profiles for pipe and channel flow, Eqs. (3.10), (3.12), (3.14), (4.11), (4.14) and (4.21)

With the linear Navier boundary condition at the inner surface of the pipe we have

$$r = 1, \quad v_z = -\ell \frac{dv_z}{dr}, \tag{3.11}$$

where $\ell = \ell^*/R > 0$ is a constant dimensionless slip length and the negative sign in front of ℓ is a reflection of Eq. (3.9), so that Eq. (3.8) becomes

$$v_z(r) = 1 - r^2 + 2\ell. \tag{3.12}$$

This profile is illustrated in Fig. 1 for $\ell = 0.5$.

With the nonlinear Navier boundary condition for the case where $\alpha > 0$ and $\beta > 0$ at the inner surface of the pipe we have

$$r = 1, \quad v_z = -\alpha \left[1 + \beta \frac{dv_z}{dr}\right]^{-\frac{1}{2}} \frac{dv_z}{dr}, \tag{3.13}$$

where $\alpha = \alpha^*/R$ and $\beta = 4\mu\beta^*/AR$ and the negative sign in front of α and the positive sign in front of β is a reflection of Eq. (3.9). Hence Eq. (3.8) becomes

$$v_z(r) = 1 - r^2 + \frac{2\alpha}{\sqrt{1 - 2\beta}}, \tag{3.14}$$

which implies $0 < \beta < 1/2$. This profile is illustrated in Fig. 1 for $\alpha = 0.5$ and $\beta = 0.1$ and $\beta = 0.4$.

4 Flow through an infinite channel

Consider the flow of an incompressible Newtonian fluid between two parallel planes of infinite extent separated by a distance $2h$. The flow is driven by a pressure difference $P_0 - P_L$ acting over a distance L parallel to the planes. A cartesian coordinate system (x^*, y^*, z^*) will be used, where x^* is measured from the midpoint between the two planes normal to the planes, while z^* is measured parallel to the planes positive in the direction of flow. A velocity distribution of the form

$$v_x^* = 0, \quad v_y^* = 0, \quad v_z^* = v_z^*(x^*), \tag{4.1}$$

is assumed such that the mass conservation equation is automatically satisfied and the momentum conservation equation is given by (see [7])

z-component:

$$0 = -\frac{\partial P^*}{\partial z^*} + \mu \frac{d^2 v_z^*}{dx^{*2}}, \tag{4.2}$$

while the x^* and y^* components yield $\partial P^*/\partial x^* = 0 = \partial P^*/\partial y^*$; thus the z^* component may be written

$$\frac{dP^*}{dz^*} = \mu \frac{d^2 v_z^*}{dx^{*2}}. \tag{4.3}$$

Since the left hand side of the above equation is a function of z^* only and the right hand side is a function of x^* only, we have

$$\frac{dP^*}{dz^*} = -A = \mu \frac{d^2 v_z^*}{dx^{*2}}, \tag{4.4}$$

where A is a constant. By applying the boundary conditions $P^* = P_0$ at $z^* = 0$ and $P^* = P_L$ at $z^* = L$, we find that

$$P^* = -Az^* + P_0, \quad A = \frac{P_0 - P_L}{L} > 0, \tag{4.5}$$

hence

$$v_z^*(x^*) = -\frac{A}{2\mu} x^{*2} + C_1^* x^* + C_2^*, \tag{4.6}$$

where C_1^* and C_2^* are integration constants to be found. By introducing the dimensionless variables

$$v_z = \frac{2\mu v_z^*}{Ah^2}, \quad x = \frac{x^*}{h}, \tag{4.7}$$

we have

$$v_z(x) = -x^2 + C_1 x + C_2. \tag{4.8}$$

Note that

$$\left.\frac{dv_z}{dx}\right|_{x=\pm 1} = \mp 2 + C_1, \tag{4.9}$$

that is, the sign of the derivative at each solid boundary depends on the value of the as yet unknown value of the integration constant C_1. There are four cases in total to consider:

$$\begin{aligned}
&\text{Case 1: } \left.\frac{dv_z}{dx}\right|_{x=1} < 0, \ \left.\frac{dv_z}{dx}\right|_{x=-1} > 0, \ \Rightarrow -2 < C_1 < 2, \\
&\text{Case 2: } \left.\frac{dv_z}{dx}\right|_{x=1} > 0, \ \left.\frac{dv_z}{dx}\right|_{x=-1} > 0, \ \Rightarrow C_1 > 2, \\
&\text{Case 3: } \left.\frac{dv_z}{dx}\right|_{x=1} < 0, \ \left.\frac{dv_z}{dx}\right|_{x=-1} < 0, \ \Rightarrow C_1 < -2, \\
&\text{Case 4: } \left.\frac{dv_z}{dx}\right|_{x=1} > 0, \ \left.\frac{dv_z}{dx}\right|_{x=-1} < 0, \ \Rightarrow C_1 > 2, \ C_1 < -2.
\end{aligned} \tag{4.10}$$

Obviously, the fourth case is impossible and need not be considered.

With a no-slip boundary condition at each solid plane we have $v_z = 0$ when $x = \pm 1$ so that Eq. (4.8) becomes

$$v_z(x) = 1 - x^2, \tag{4.11}$$

and again this is the standard parabolic profile shown in Fig. 1.

4.1 Solution with linear Navier boundary condition

a. Case 1

With the linear Navier boundary condition for the case where ℓ^* assumes contant and equal values at each solid plane we have

$$x = \pm 1, \quad v_z = \mp \ell \frac{dv_z}{dx}, \tag{4.12}$$

where $\ell = \ell^*/h > 0$ is a constant dimensionless slip length, so that

$$C_1 = 0, \quad C_2 = 1 + 2\ell, \tag{4.13}$$

which clearly satisfies the requirement of Eq. (4.10), so that Eq. (4.8) becomes

$$v_z(x) = 1 - x^2 + 2\ell. \tag{4.14}$$

This profile is illustrated in Fig. 1 for $\ell = 0.5$.

b. Case 2

For this case we have

$$x = \pm 1, \quad v_z = \ell \frac{dv_z}{dx}, \tag{4.15}$$

so that

$$C_1 = -2\ell, \quad C_2 = 1 - 2\ell^2, \tag{4.16}$$

which clearly does not satisfy the requirement of Eq. (4.10) for $\ell > 0$.

c. Case 3

For this case we have

$$x = \pm 1, \quad v_z = -\ell \frac{dv_z}{dx}, \tag{4.17}$$

so that

$$C_1 = 2\ell, \quad C_2 = 1 - 2\ell^2, \tag{4.18}$$

which clearly does not satisfy the requirement of Eq. (4.10) for $\ell > 0$.

4.2 Solution with nonlinear Navier boundary condition

a. Case 1

With the nonlinear Navier boundary condition for the case where $\alpha > 0$ and $\beta > 0$ at each solid plane are equal we have

$$x = \pm 1, \quad v_z = \mp\alpha\left[1 \pm \beta\frac{dv_z}{dx}\right]^{-\frac{1}{2}}\frac{dv_z}{dx}, \tag{4.19}$$

where $\alpha = \alpha^*/h$ and $\beta = 2\mu\beta^*/Ah$. Substituting the general solution (4.8) into the boundary conditions and solving for C_2 yields

$$\begin{aligned} C_2 &= 1 - C_1 - \frac{\alpha(C_1 - 2)}{\sqrt{1 + \beta(C_1 - 2)}}, \\ C_2 &= 1 + C_1 + \frac{\alpha(C_1 + 2)}{\sqrt{1 - \beta(C_1 + 2)}}. \end{aligned} \tag{4.20}$$

These two expressions are equivalent, so that subtracting one from the other gives an equation equal to zero, which must be solved for $|C_1| < 2$. It is obvious that $C_1 = 0$ is a solution, and for this case Eq. (4.8) becomes

$$v_z(x) = 1 - x^2 + \frac{2\alpha}{\sqrt{1 - 2\beta}}, \tag{4.21}$$

which implies $0 < \beta < 1/2$. This profile is illustrated in Fig. 1 for $\alpha = 0.5$ and $\beta = 0.1$ and $\beta = 0.4$.

To investigate if there are other solutions, we subtract Eqs. (4.20) from each other and solve for $\alpha > 0$, which gives for $C_1 \neq 0$

$$\begin{aligned} \alpha = -\Big[2C_1\sqrt{1 + \beta(C_1 - 2)}\sqrt{1 - \beta(C_1 + 2)}\Big] \Big/ \Big[C_1\Big(\sqrt{1 + \beta(C_1 - 2)} \\ + \sqrt{1 - \beta(C_1 + 2)}\Big) + 2\Big(\sqrt{1 + \beta(C_1 - 2)} - \sqrt{1 - \beta(C_1 + 2)}\Big)\Big]. \end{aligned} \tag{4.22}$$

Now, we require the square roots and the terms inside the square roots to be positive, which implies $0 < \beta < 1/(2 + |C_1|)$. If $0 < C_1 < 2$ then we have

$$\sqrt{1 + \beta(C_1 - 2)} - \sqrt{1 - \beta(C_1 + 2)} > 0, \tag{4.23}$$

so that both the numerator and denominator of Eq. (4.22) are positive, and hence $\alpha < 0$, which is a contradiction. If $-2 < C_1 < 0$ then we have

$$\sqrt{1 + \beta(C_1 - 2)} - \sqrt{1 - \beta(C_1 + 2)} < 0, \tag{4.24}$$

so that both the numerator and denominator of Eq. (4.22) are negative, and hence $\alpha < 0$, which is again a contradiction. Hence $C_1 = 0$ is the only valid solution.

b. Case 2

For this case we have

$$x = \pm 1, \quad v_z = \alpha\left[1 - \beta\frac{dv_z}{dx}\right]^{-\frac{1}{2}}\frac{dv_z}{dx}. \tag{4.25}$$

Substituting the general solution (4.8) into the boundary conditions and solving for C_2 yields

$$\begin{aligned} C_2 &= 1 - C_1 + \frac{\alpha(C_1 - 2)}{\sqrt{1 - \beta(C_1 - 2)}}, \\ C_2 &= 1 + C_1 + \frac{\alpha(C_1 + 2)}{\sqrt{1 - \beta(C_1 + 2)}}. \end{aligned} \tag{4.26}$$

These two expressions are equivalent, so that subtracting one from the other gives an equation equal to zero, which must be solved for $C_1 > 2$. Solving for $\alpha > 0$ gives

$$\alpha = -\Big[2C_1\sqrt{1-\beta(C_1-2)}\sqrt{1-\beta(C_1+2)}\Big] \Big/ \Big[C_1\Big(\sqrt{1-\beta(C_1-2)} - \sqrt{1-\beta(C_1+2)}\Big) + 2\Big(\sqrt{1-\beta(C_1-2)} + \sqrt{1-\beta(C_1+2)}\Big)\Big]. \tag{4.27}$$

Now, again we require the square roots and the terms inside the square roots to be positive, which implies $0 < \beta < 1/(2 + C_1)$. For $C_1 > 2$ we have

$$\sqrt{1-\beta(C_1-2)} - \sqrt{1-\beta(C_1+2)} > 0, \tag{4.28}$$

so that both the numerator and denominator of Eq. (4.27) are positive, and hence $\alpha < 0$, which is a contradiction. Hence there are no valid solutions for this case.

c. Case 3

For this case we have

$$x = \pm 1, \quad v_z = -\alpha\left[1 + \beta\frac{dv_z}{dx}\right]^{-\frac{1}{2}}\frac{dv_z}{dx}. \tag{4.29}$$

Substituting the general solution Eq. (4.8) into the boundary conditions and solving for C_2 yields

$$\begin{aligned} C_2 &= 1 - C_1 - \frac{\alpha(C_1-2)}{\sqrt{1+\beta(C_1-2)}}, \\ C_2 &= 1 + C_1 - \frac{\alpha(C_1+2)}{\sqrt{1+\beta(C_1+2).}} \end{aligned} \tag{4.30}$$

These two expressions are equivalent, so that subtracting one from the other gives an equation equal to zero, which must be solved for $C_1 < -2$. Solving for $\alpha > 0$ gives

$$\alpha = -\Big[2(-C_1)\sqrt{1+\beta(C_1+2)}\sqrt{1+\beta(C_1-2)}\Big] \Big/ \Big[(-C_1)\Big(\sqrt{1+\beta(C_1+2)} - \sqrt{1+\beta(C_1-2)}\Big) + 2\Big(\sqrt{1+\beta(C_1+2)} + \sqrt{1+\beta(C_1-2)}\Big)\Big]. \tag{4.31}$$

Again, we require the square roots and the terms inside the square roots to be positive, which implies $0 < \beta < 1/(2 - C_1)$. For $C_1 < -2$ we have

$$\sqrt{1+\beta(C_1+2)} - \sqrt{1+\beta(C_1-2)} > 0, \tag{4.32}$$

so that both the numerator and denominator of Eq. (4.31) are positive, and hence $\alpha < 0$, which is a contradiction. Hence there are no valid solutions for this case.

5 Flow through an infinite annulus

Consider the steady flow of an incompressible Newtonian fluid through the annular region between two infinite coaxial pipes of radii R and κR, where $0 < \kappa < 1$. The flow is driven by a

pressure difference $P_0 - P_L$ acting over a distance L parallel to the two pipes. A cylindrical coordinate system (r^*, θ, z^*) will be used, where r^* is measured in the radial direction and z^* is measured in the axial direction positive in the direction of flow. A velocity distribution of the form in Sect. 3 is assumed, so that the general solution is given by

$$v_z(r) = -r^2 + C_1 + C_2 \ln r. \tag{5.1}$$

Note that

$$\left.\frac{dv_z}{dr}\right|_{r=1} = -2 + C_2, \quad \left.\frac{dv_z}{dr}\right|_{r=\kappa} = -2\kappa + \frac{C_2}{\kappa}, \tag{5.2}$$

that is, the sign of the derivative at each solid boundary depends on the value of the as yet unknown value of the integration constant C_2. There are four cases in total to consider:

$$\begin{aligned}
&\text{Case 1: } \left.\frac{dv_z}{dr}\right|_{r=1} < 0, \quad \left.\frac{dv_z}{dr}\right|_{r=\kappa} > 0, \Rightarrow 2\kappa^2 < C_2 < 2,\\
&\text{Case 2: } \left.\frac{dv_z}{dr}\right|_{r=1} > 0, \quad \left.\frac{dv_z}{dr}\right|_{r=\kappa} > 0, \Rightarrow C_2 > 2,\\
&\text{Case 3: } \left.\frac{dv_z}{dr}\right|_{r=1} < 0, \quad \left.\frac{dv_z}{dr}\right|_{r=\kappa} < 0, \Rightarrow C_2 < 2\kappa^2,\\
&\text{Case 4: } \left.\frac{dv_z}{dr}\right|_{r=1} > 0, \quad \left.\frac{dv_z}{dr}\right|_{r=\kappa} < 0, \Rightarrow C_2 > 2,\ C_2 < 2\kappa^2.
\end{aligned} \tag{5.3}$$

Obviously, the fourth case is impossible and need not be considered.

With a no-slip boundary condition at the inner surface of the outer pipe and outer surface of the inner pipe we have $v_z = 0$ when $r = \kappa$ and $r = 1$ so that Eq. (5.1) becomes

$$v_z(r) = 1 - r^2 + \frac{1 - \kappa^2}{\ln(\kappa^{-1})} \ln r. \tag{5.4}$$

This profile is illustrated in Fig. 2 for $\kappa = 0.5$.

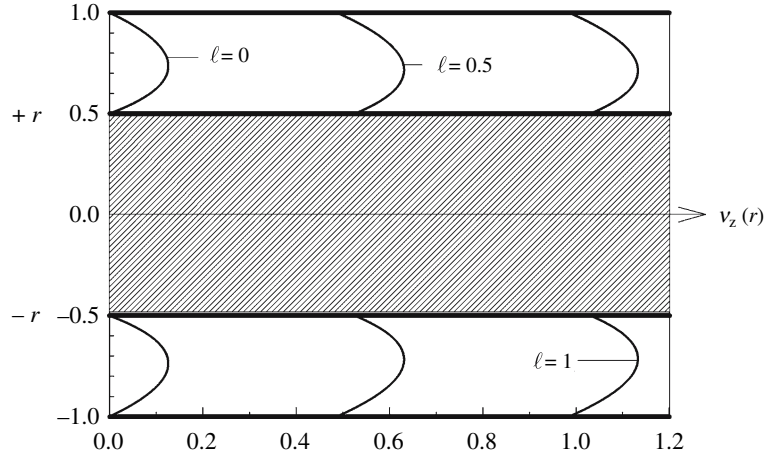

Fig. 2. Velocity profiles for annulus flow, Eqs. (5.4) and (5.7)

5.1 Solution with linear Navier boundary condition

a. Case 1

With the linear Navier boundary condition at the inner surface of the outer pipe and outer surface of the inner pipe we have

$$\begin{aligned} r &= 1, \quad v_z = -\ell \frac{dv_z}{dr}, \\ r &= \kappa, \quad v_z = \ell \frac{dv_z}{dr}, \end{aligned} \tag{5.5}$$

where $\ell = \ell^*/R > 0$ is a constant dimensionless slip length, so that

$$\begin{aligned} C_1 &= \frac{\left[\kappa \ln\left(\kappa^{-1}\right) + \ell\right](1+2\ell) + \ell\kappa^2(\kappa - 2\ell)}{\kappa \ln(\kappa^{-1}) + \ell(1+\kappa)}, \\ C_2 &= \frac{\kappa(1+\kappa)[1-\kappa+2\ell]}{\kappa \ln(\kappa^{-1}) + \ell(1+\kappa)}, \end{aligned} \tag{5.6}$$

which satisfies the requirement of Eq. (5.3) as illustrated in Figs. 3 and 4 for $\ell = 0.5$ and $\ell = 1$, respectively, so that Eq. (5.1) becomes

$$\begin{aligned} v_z(r) = &\frac{\left[\kappa \ln\left(\kappa^{-1}\right) + \ell\right](1+2\ell) + \ell\kappa^2(\kappa - 2\ell)}{\kappa \ln(\kappa^{-1}) + \ell(1+\kappa)} - r^2 \\ &+ \frac{\kappa(1+\kappa)[1-\kappa+2\ell]}{\kappa \ln(\kappa^{-1}) + \ell(1+\kappa)} \ln r. \end{aligned} \tag{5.7}$$

This profile is illustrated in Fig. 2 for $\kappa = 0.5$ and $\ell = 0.5$ and $\ell = 1$.

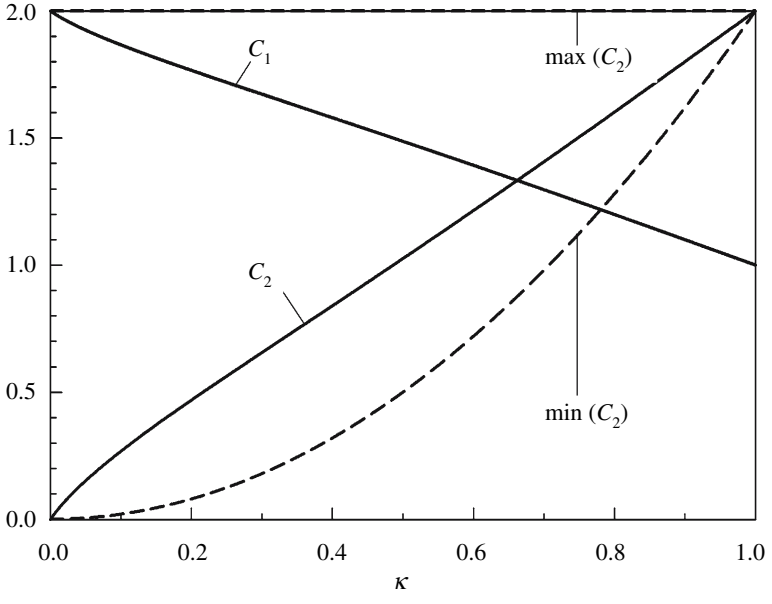

Fig. 3. Integration constants for annulus flow, Eq. (5.6) for $2\kappa^2 < C_2 < 2$ and $\ell = 0.5$

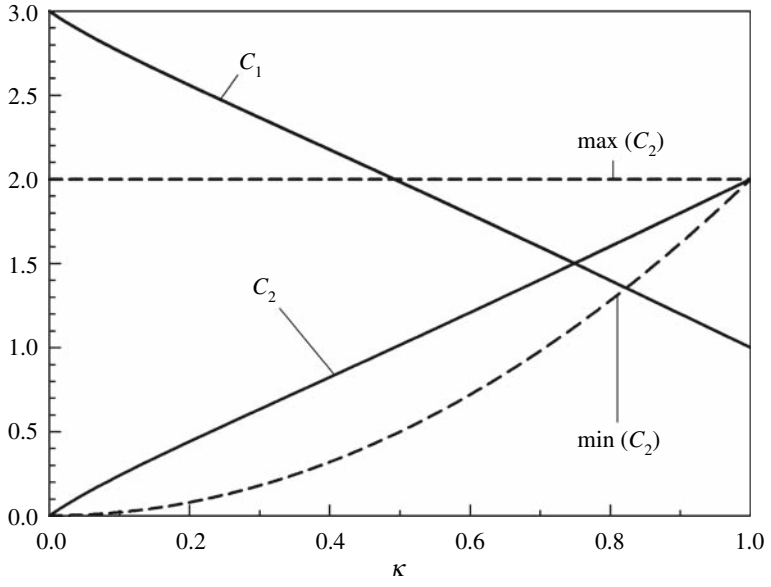

Fig. 4. Integration constants for annulus flow, Eq. (5.6) for $2\kappa^2 < C_2 < 2$ and $\ell = 1$

b. Case 2

For this case we have

$$\begin{aligned} r = 1, \quad v_z &= \ell \frac{dv_z}{dr}, \\ r = \kappa, \quad v_z &= \ell \frac{dv_z}{dr}, \end{aligned} \tag{5.8}$$

so that

$$\begin{aligned} C_1 &= \frac{\left[\kappa \ln\left(\kappa^{-1}\right) + \ell\right](1 - 2\ell) - \ell\kappa^2(\kappa - 2\ell)}{\kappa \ln(\kappa^{-1}) + \ell(1 - \kappa)}, \\ C_2 &= \frac{\kappa(1 - \kappa)[1 + \kappa - 2\ell]}{\kappa \ln(\kappa^{-1}) + \ell(1 - \kappa)}, \end{aligned} \tag{5.9}$$

which does not satisfy the requirement of Eq. (5.3) for all $\ell > 0$ and $0 < \kappa < 1$, an example of which is shown in Fig. 5 for $\ell = 0.5$.

c. Case 3

For this case we have

$$\begin{aligned} r = 1, \quad v_z &= -\ell \frac{dv_z}{dr}, \\ r = \kappa, \quad v_z &= -\ell \frac{dv_z}{dr}, \end{aligned} \tag{5.10}$$

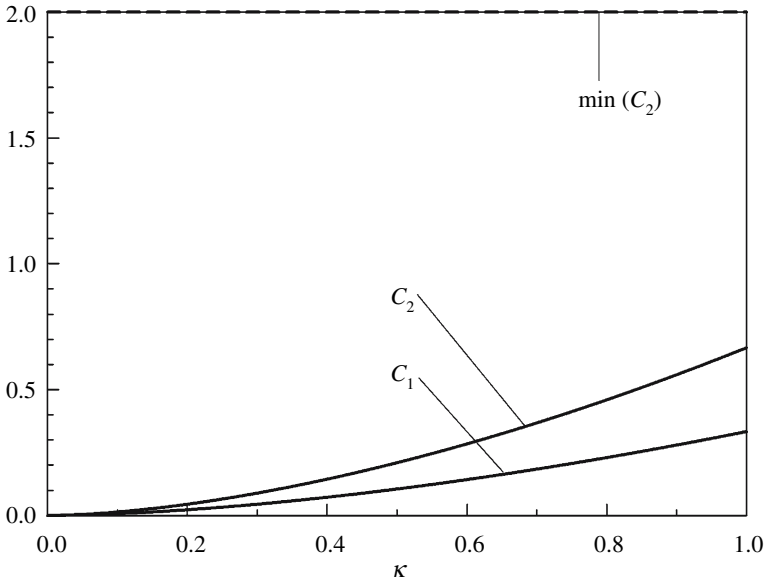

Fig. 5. Integration constants for annulus flow, Eq. (5.9) for $C_2 > 2$ and $\ell = 0.5$

so that

$$C_1 = \frac{\left[\kappa \ln\left(\kappa^{-1}\right) - \ell\right](1+2\ell) + \ell\kappa^2(\kappa+2\ell)}{\kappa \ln(\kappa^{-1}) - \ell(1-\kappa)},$$
$$C_2 = \frac{\kappa(1-\kappa)[1+\kappa+2\ell]}{\kappa \ln(\kappa^{-1}) - \ell(1-\kappa)}, \tag{5.11}$$

for

$$\ell \neq \frac{\kappa \ln\left(\kappa^{-1}\right)}{1-\kappa}. \tag{5.12}$$

Since

$$0 < \frac{\kappa \ln\left(\kappa^{-1}\right)}{1-\kappa} < 1, \tag{5.13}$$

for $0 < \kappa < 1$, for $\ell > 1$ the requirement of Eq. (5.3) will always be satisfied, while for $0 < \ell < 1$ the requirement of Eq. (5.3) will only be satisfied for a particular range of κ. This is illustrated in Fig. 6, which plots the integration constants C_1 and C_2 for $\ell = 0.5$. For this case

$$\frac{\kappa \ln\left(\kappa^{-1}\right)}{1-\kappa} = 0.5 \Rightarrow \kappa = 0.285, \tag{5.14}$$

so that for $0 < \kappa < 0.285$, $C_2 < 2\kappa^2$. Figure 7 plots the integration constants C_1 and C_2 for $\ell = 2$, demonstrating that $C_2 < 2\kappa^2$ for all κ. The velocity profile is thus given by

$$v_z(r) = \frac{\left[\kappa \ln\left(\kappa^{-1}\right) - \ell\right](1+2\ell) + \ell\kappa^2(\kappa+2\ell)}{\kappa \ln(\kappa^{-1}) - \ell(1-\kappa)} - r^2$$
$$+ \frac{\kappa(1-\kappa)[1+\kappa+2\ell]}{\kappa \ln(\kappa^{-1}) - \ell(1-\kappa)} \ln r \tag{5.15}$$

and is illustrated in Fig. 8 for $\kappa = 0.25$ and $\ell = 0.5$ and $\ell = 2$.

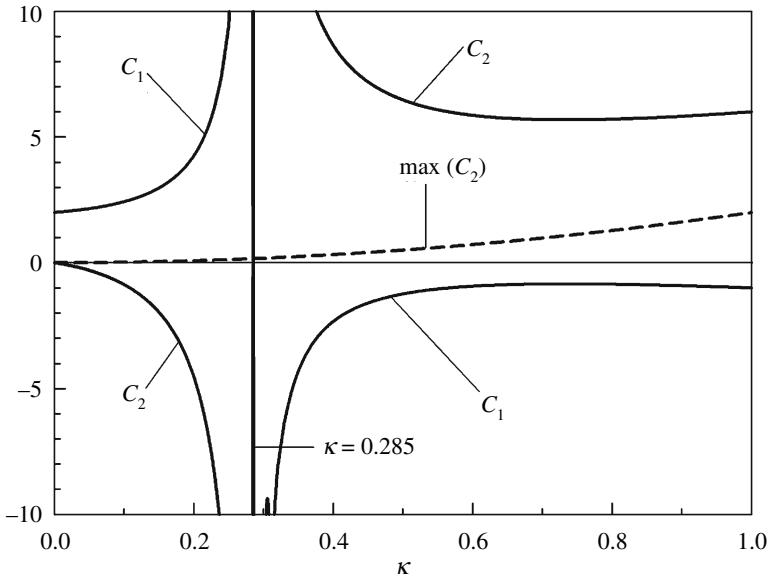

Fig. 6. Integration constants for annulus flow, Eq. (5.11) for $C_2 < 2\kappa^2$ and $\ell = 0.5$

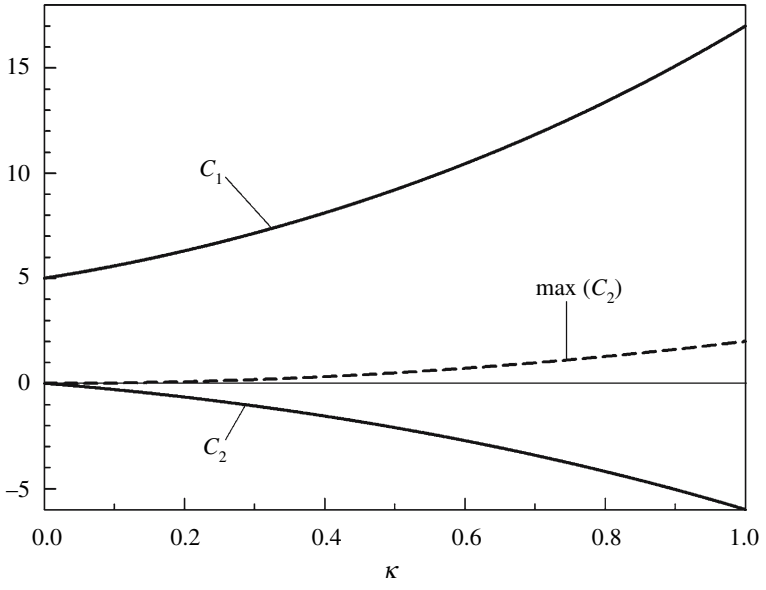

Fig. 7. Integration constants for annulus flow, Eq. (5.11) for $C_2 < 2\kappa^2$ and $\ell = 2$

5.2 Solution with nonlinear Navier boundary condition

a. Case 1

With the nonlinear Navier boundary condition for the case where $\alpha > 0$ and $\beta > 0$ at the inner surface of the outer pipe and outer surface of the inner pipe we have

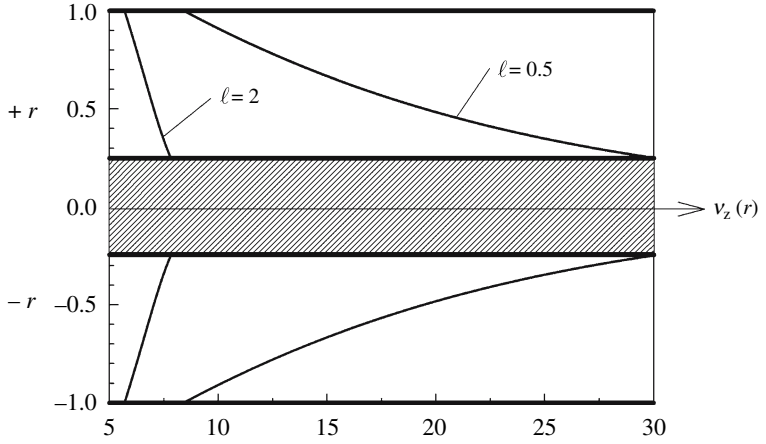

Fig. 8. Velocity profiles for annulus flow, Eq. (5.15) for $\kappa = 0.5$

$$
\begin{aligned}
&r = 1, \quad v_z = -\alpha\left[1 + \beta\frac{dv_z}{dr}\right]^{-\frac{1}{2}}\frac{dv_z}{dr}, \\
&r = \kappa, \quad v_z = \alpha\left[1 - \beta\frac{dv_z}{dr}\right]^{-\frac{1}{2}}\frac{dv_z}{dr},
\end{aligned}
\tag{5.16}
$$

where $\alpha = \alpha^*/R$ and $\beta = 4\mu\beta^*/AR$. Substituting the general solution (5.1) into the boundary conditions and solving for C_1 yields

$$
\begin{aligned}
&C_1 = 1 - \frac{\alpha(C_2 - 2)}{\sqrt{1 + \beta(C_2 - 2)}}, \\
&C_1 = \kappa^2 + C_2\ln\left(\kappa^{-1}\right) + \frac{\alpha\left(C_2 - 2\kappa^2\right)}{\sqrt{\kappa[\kappa - \beta(C_2 - 2\kappa^2)]}},
\end{aligned}
\tag{5.17}
$$

which must be solved for $2\kappa^2 < C_2 < 2$. For the terms inside the square roots to remain positive we require

$$\beta < \frac{1}{2 - C_2} \tag{5.18}$$

for $2\kappa^2 < C_2 < 2\kappa$, and

$$\beta < \frac{\kappa}{C_2 - 2\kappa^2} \tag{5.19}$$

for $2\kappa < C_2 < 2$. Solutions are found by generating plots of C_1 versus C_2 for given values of κ, α and β for each expression. It is found that there is only one solution for each set of κ, α and β. The results for $\kappa = 0.5$, $\alpha = 1$ and $\beta = 0.25$ are shown in Fig. 9, which has the solution $C_1 = 1.01$ and $C_2 = 2.14$.

By subtracting Eqs. (5.17) from each other we obtain an expression free of C_1, which may be solved for set values of κ and α and varying β up to the maximum value of β, $\beta_{\max}$, as given by Eqs. (5.18) and (5.19) (whichever is smaller). Figure 10 shows a plot of the solutions for C_1 and C_2 for $\kappa = 0.5$ and $\alpha = 1$ for β ranging from 0 to $\beta_{\max} = 1$. Figure 11 plots the velocity profiles for $\kappa = 0.5$, $\alpha = 1$ and $\beta = 0.25$, 0.5 and 0.75.

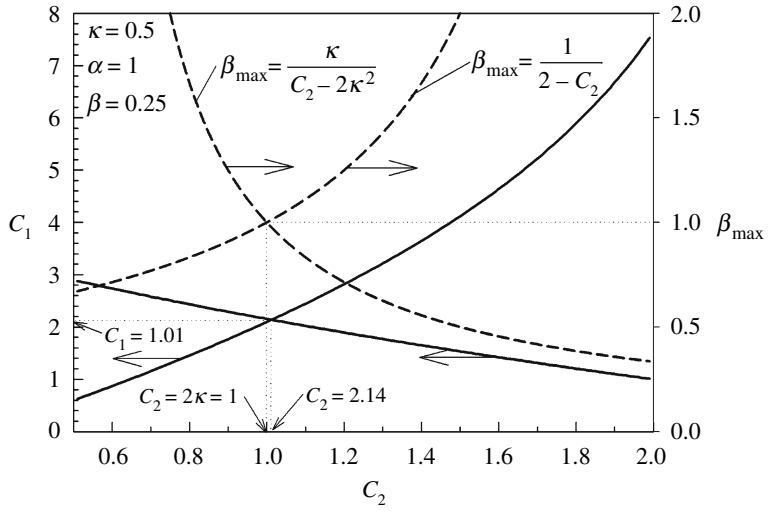

Fig. 9. Integration constants for annulus flow, Eq. (5.17) for $2\kappa^2 < C_2 < 2$ and $\kappa = 0.5$, $\alpha = 1$ and $\beta = 0.25$

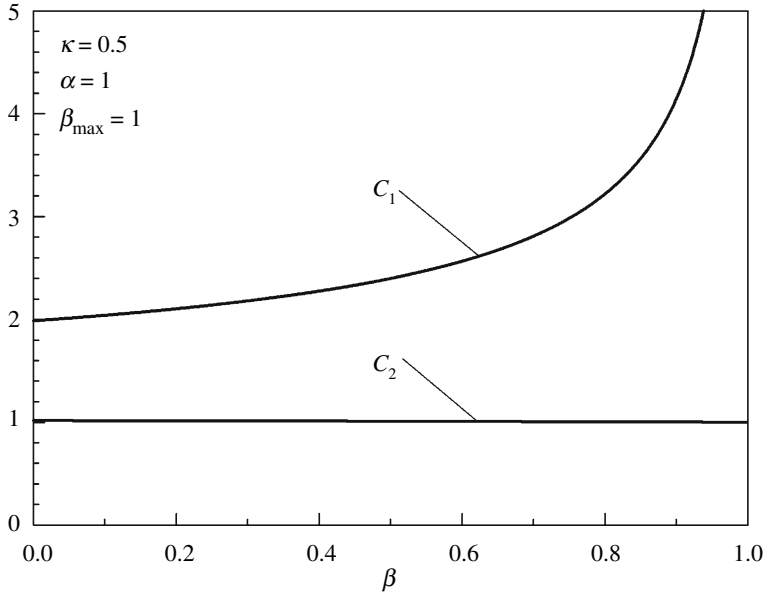

Fig. 10. Integration constants for annulus flow, Eq. (5.17) for $2\kappa^2 < C_2 < 2$ and $\kappa = 0.5$, $\alpha = 1$ and $0 < \beta < \beta_{\max} = 1$

b. Case 2

For this case we have

$$r = 1, \quad v_z = \alpha\left[1 - \beta\frac{dv_z}{dr}\right]^{-\frac{1}{2}}\frac{dv_z}{dr},$$
$$r = \kappa, \quad v_z = \alpha\left[1 - \beta\frac{dv_z}{dr}\right]^{-\frac{1}{2}}\frac{dv_z}{dr}. \tag{5.20}$$

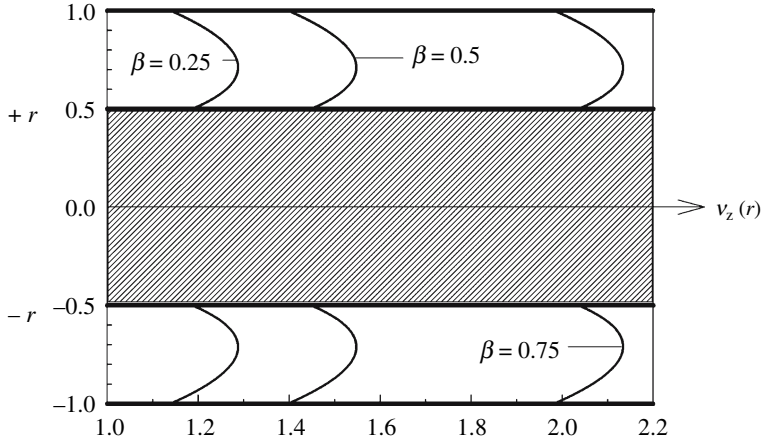

Fig. 11. Velocity profiles for annulus flow, Eq. (5.1) for $\kappa = 0.5$ and $\alpha = 1$

Substituting the general solution (5.1) into the boundary conditions and solving for C_1 yields

$$C_1 = 1 + \frac{\alpha(C_2 - 2)}{\sqrt{1 - \beta(C_2 - 2)}},$$
$$C_1 = \kappa^2 + C_2 \ln\left(\kappa^{-1}\right) + \frac{\alpha\left(C_2 - 2\kappa^2\right)}{\sqrt{\kappa[\kappa - \beta(C_2 - 2\kappa^2)]}}, \tag{5.21}$$

which must be solved for $C_2 > 2$. For the terms inside the square roots to remain positive we require

$$\beta < \frac{\kappa}{C_2 - 2\kappa^2} \tag{5.22}$$

for $C_2 > 2$. Solutions are found by generating plots of C_1 versus C_2 for given values of κ, α and β for each expression. It is found that there are no solutions for each set of κ, α and β. The results for $\kappa = 0.5$, $\alpha = 1$ and $\beta = 0.1$ are shown in Fig. 12.

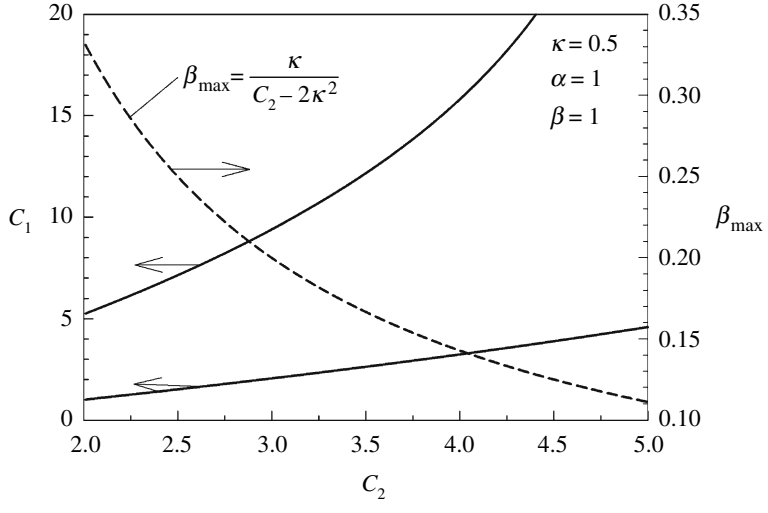

Fig. 12. Integration constants for annulus flow, Eq. (5.21) for $C_2 > 2$ and $\kappa = 0.5$, $\alpha = 1$ and $\beta = 0.1$

c. Case 3

For this case we have

$$r = 1, \quad v_z = -\alpha\left[1 + \beta\frac{dv_z}{dr}\right]^{-\frac{1}{2}}\frac{dv_z}{dr},$$
$$r = \kappa, \quad v_z = -\alpha\left[1 + \beta\frac{dv_z}{dr}\right]^{-\frac{1}{2}}\frac{dv_z}{dr}. \tag{5.23}$$

Substituting the general solution Eq. (5.1) into the boundary conditions and solving for C_1 yields

$$C_1 = 1 - \frac{\alpha(C_2 - 2)}{\sqrt{1 + \beta(C_2 - 2)}},$$
$$C_1 = \kappa^2 + C_2\ln\left(\kappa^{-1}\right) - \frac{\alpha\left(C_2 - 2\kappa^2\right)}{\sqrt{\kappa[\kappa + \beta(C_2 - 2\kappa^2)]}}, \tag{5.24}$$

which must be solved for $C_2 < 2\kappa^2$. For the terms inside the square roots to remain positive we require

$$\beta < \frac{1}{2 - C_2} \tag{5.25}$$

for $-2\kappa < C_2 < 2\kappa$, and

$$\beta < \frac{\kappa}{2\kappa^2 - C_2} \tag{5.26}$$

for $C_2 < -2\kappa$. Solutions are found by generating plots of C_1 versus C_2 for given values of κ, α and β for each expression. It is found that there is only one solution for each set of κ, α and β. Recall that for the linear case for $\ell < 1$, that is $\alpha < 1$, solutions were only generated for a particular range of κ. The results for $\kappa = 0.5$, $\alpha = 0.5$ and $\beta = 0.1$ are shown in Fig. 13, which has solution $C_1 = 4.52$ and $C_2 = -2.99$.

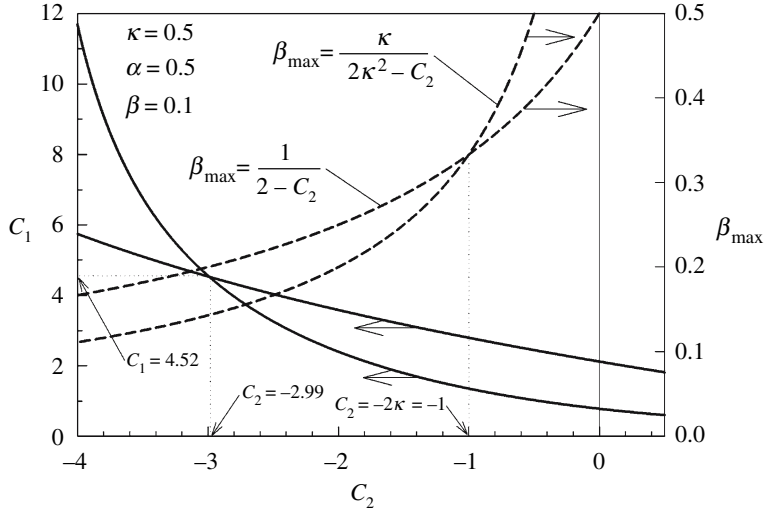

Fig. 13. Integration constants for annulus flow, Eq. (5.24) for $C_2 < 2\kappa^2$ and $\kappa = 0.5$, $\alpha = 0.5$ and $\beta = 0.1$

By subtracting Eqs. (5.24) from each other we obtain an expression free of C_1, which may be solved for set values of κ and α and varying β up to the maximum value of β, $\beta_{\max}$, as given by Eqs. (5.25) and (5.26) (whichever is smaller). Figure 14 shows a plot of the solutions for C_1 and C_2 for $\kappa = 0.5$ and $\alpha = 0.5$ for β ranging from 0 to $\beta_{\max} = 0.15$. Figure 15 plots the velocity profiles for $\kappa = 0.5$ and $\alpha = 0.5$.

The results for $\kappa = 2$, $\alpha = 0.5$ and $\beta = 0.2$ are shown in Fig. 16, which has solution $C_1 = 11.85$ and $C_2 = -1.23$. Figure 17 shows a plot of the solutions for C_1 and C_2 for $\kappa = 0.5$ and $\alpha = 2$ for β ranging from 0 to $\beta_{\max} = 0.33$. Figure 15 plots the velocity profiles for $\kappa = 0.5$ and $\alpha = 0.5$.

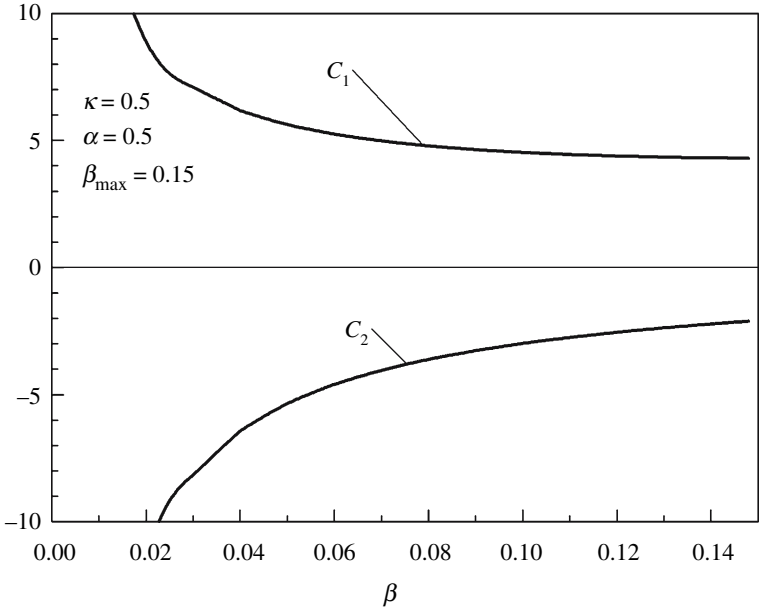

Fig. 14. Integration constants for annulus flow, Eq. (5.24) for $C_2 < 2\kappa^2$ and $\kappa = 0.5$, $\alpha = 0.5$ and $0 < \beta < \beta_{\max} = 0.15$

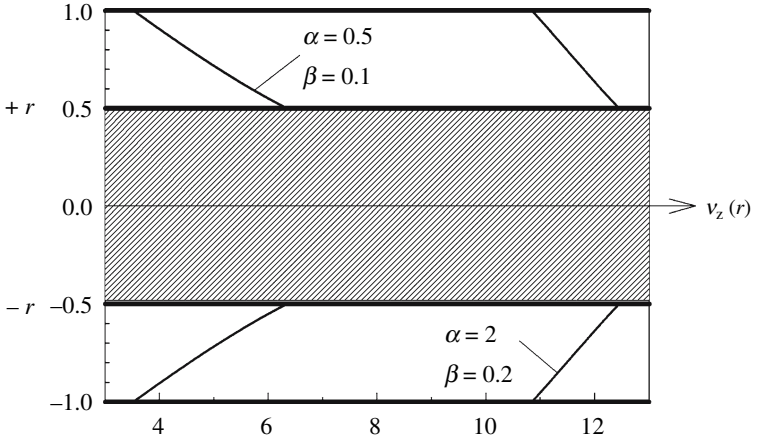

Fig. 15. Velocity profiles for annulus flow, Eq. (5.1) for $\kappa = 0.5$

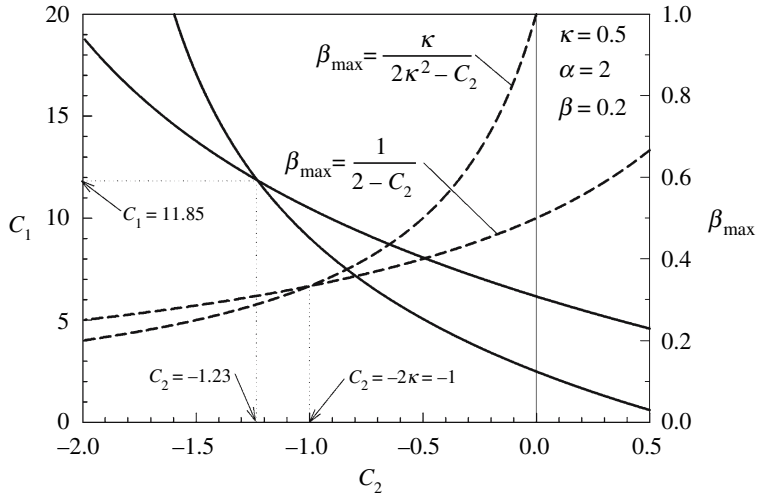

Fig. 16. Integration constants for annulus flow, Eq. (5.24) for $C_2 < 2\kappa^2$ and $\kappa = 0.5$, $\alpha = 2$ and $\beta = 0.2$

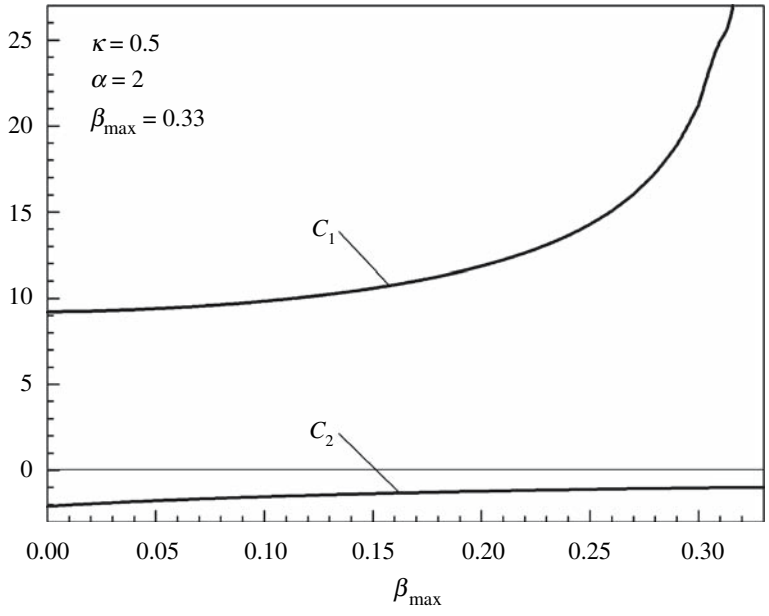

Fig. 17. Integration constants for annulus flow, Eq. (5.24) for $C_2 < 2\kappa^2$ and $\kappa = 0.5$, $\alpha = 2$ and $0 < \beta < \beta_{max} = 0.33$

6 Results and conclusions

Although the boundary condition proposed by Thompson and Troian [35] is highly nonlinear and possibly singular, the results presented here for three simple pressure-driven flows through a pipe, a channel and an annulus suggest that in terms of the assumed form of the solution the integration constants obtained are still unique when care is taken concerning the sign of

the normal derivative of velocity at the boundary. When there is only one boundary on which the condition is applied, as for the flow through a pipe, the results are simple and are seen to be unique immediately.

When there are two boundaries on which the condition is applied, as with the flow through a channel and an annulus, complicated transcendental equations are obtained for the integration constants, which on first inspection may appear to offer multiple solutions. However, careful delineation of the various signs of the constants involved in the nonlinear Navier boundary condition suggests that for the assumed form of the solution uniqueness is maintained.

For the flow through the pipe and channel, a careful examination of the sign of the normal derivative of velocity at the boundary and of the constants involved in the nonlinear Navier boundary condition indicates that there is only one acceptable solution of the assumed form, which for these one-dimensional problems behave like a modified slip length, ℓ_m say, in the Navier boundary condition; that is if ℓ_m is defined via

$$\ell_m = \frac{\alpha}{\sqrt{1-2\beta}}, \tag{6.1}$$

where α and β are the non-dimensional constants associated with the nonlinear Navier boundary condition. If this definition of the slip length is applied to the linear Navier boundary condition (which may no longer be of small magnitude, since $\ell_m \to \infty$ as $\beta \to 1/2$), then the solutions obtained agree with those for the nonlinear Navier boundary condition.

The solutions for the pressure-driven flow through an annulus are quite different to those for the pipe and the channel. Two distinct cases for the sign of the normal derivative of velocity at each boundary are obtained, which produce two solutions for both the linear and nonlinear Navier boundary conditions which are mathematically and physically acceptable. One set of these solutions corresponds to the standard parabolic profile with an increased maximum for positive values of the slip length (for the linear case) and positive constants (for the nonlinear Navier boundary condition). The other solution is for the case where the normal derivative of velocity at each boundary is negative. Here the predicted profile is monotone and predicts that the slip velocity is much greater at the outer surface of the inner pipe than at the inner surface of the outer pipe. For the linear Navier boundary condition the results demonstrate that when the slip length $\ell > 1$ solutions may be found for the whole range of κ, which is the ratio of the radius of the smaller pipe to that of the larger pipe, while for $\ell < 1$ solutions are found for a range of κ from zero to the solution of

$$\ell(1-\kappa) - \kappa \ln\left(\kappa^{-1}\right) = 0. \tag{6.2}$$

For the nonlinear Navier boundary condition the same situation arises for $\alpha > 1$ and $\alpha < 1$, but the range of κ for $\alpha < 1$ increases as β increases from zero.

Acknowledgements

This work is funded by the Discovery Project scheme of the Australian Research Council, and the authors gratefully acknowledge this support. JMH is grateful to the Australian Research Council for provision of an Australian Professorial Fellowship.

References

[1] Gad-el-Hak, M.: The fluid mechanics of microdevices – the Freeman scholar lecture. J. Fluids Engng **121**, 5–33 (1999).
[2] Granick, S.: Motions and relaxations of confined liquids. Science **253**, 1374–1379 (1991).
[3] Granick, S.: Soft matter in a tight spot. Phys. Today **52**, 26–31 (1999).
[4] Bhushan, B., Israelachvili, J. N., Landman, U.: A nanotribology: friction, wear and lubrication at the atomic scale. Nature **374**, 607–616 (1995).
[5] Lamb, H.: Hydrodynamics. Cambridge University Press 1932.
[6] Batchelor, G. K.: An introduction to fluid dynamics. Cambridge University Press 2000.
[7] Slattery, J. C.: Advanced transport phenomena. Cambridge University Press 1999.
[8] Pit, R., Hervet, H., Léger, L.: Friction and slip of a simple liquid at a solid surface. Tribol. Lett. **7**, 147–152 (1999).
[9] Pit, R., Hervet, H., Léger, L.: Direct experimental evidence of slip in hexadecane: solid interfaces. Phys. Rev. Lett. **85**, 980–983 (2000).
[10] Craig, V. S. J., Neto, C., Williams, D. R. M.: Shear-dependent boundary slip in an aqueous Newtonian liquid. Phys. Rev. Lett. **87**, 054504 (2001).
[11] Zhu, Y., Granick, S.: Rate-dependent slip of Newtonian liquid at smooth surfaces. Phys. Rev. Lett. **87**, 096105 (2001).
[12] Zhu, Y., Granick, S.: Limits of the hydrodynamic no-slip boundary condition. Phys. Rev. Lett. **88**, 106102 (2002).
[13] Zhu, Y., Granick, S.: No-slip boundary condition switches to partial slip when fluid contains surfactant. Langmuir **18**, 10058–10063 (2002).
[14] Tretheway, D. C., Meinhart, C. D.: Apparent fluid slip at hydrophobic microchannel walls. Phys. Fluids **14**, L9–L12 (2002).
[15] Gad-el-Hak, M.: Transport phenomena in microdevices. ZAMM **84**, 494–498 (2004).
[16] Dussan, V. E. B.: The moving contact line: the slip boundary condition. J. Fluid Mech. **77**, 665–684 (1976).
[17] Dussan, V. E. B.: On the spreading of liquids on solid surfaces: static and dynamic contact lines. Ann. Rev. Fluid Mech. **11**, 371–400 (1979).
[18] Thompson, P. A., Robbins, M. O.: Simulations of contact-line motion: slip and the dynamic contact angle. Phys. Rev. Lett. **63**, 766–769 (1989).
[19] Thompson, P. A., Robbins, M. O.: Shear flow near solids: epitaxial order and flow boundary conditions. Phys. Rev. A. **41**, 6830–6837 (1990).
[20] Matthews, M. T., Hill, J. M.: Micro/nano sliding plate problem with Navier boundary condition. ZAMP **57**, 875–903 (2006).
[21] Moffatt, H. K.: Viscous and resistive eddies near a sharp corner. J. Fluid Mech. **18**, 1–18 (1963).
[22] Koplik, J., Banavar, J. R.: Corner flow in the sliding plate problem. Phys. Fluids **7**, 3118–3125 (1995).
[23] Richardson, S.: On the no-slip boundary condition. J. Fluid Mech. **59**, 707–719 (1973).
[24] Goldshtik, M. A.: Viscous flow paradoxes. Ann. Rev. Fluid Mech. **22**, 441–472 (1990).
[25] Navier, C. L. M. H.: Mémoire sur les lois du mouvement des fluides. Mémoires de l'Académie Royale des Sciences de l'Institut de France **6**, 389–440 (1823).
[26] Maxwell, J. C.: On stresses in rarefied gases arising from inequalities of temperature. Phil. Trans. R. Soc. London **170**, 231–256 (1879).
[27] Matthews, M. T., Hill, J. M.: Flow around nanospheres and nanocylinders. Q. J. Mech. Appl. Math. **59**, 191–210 (2006).
[28] Shikhmurzaev, Y. D.: The moving contact line on a smooth solid surface. Int. J. Multiph. Flow **19**, 589–610 (1993).
[29] Shikhmurzaev, Y. D.: Moving contact lines in liquid/liquid/solid systems. J. Fluid Mech. **334**, 211–249 (1997).
[30] Qian, T., Wang, X. P.: Driven cavity flow: from molecular dynamics to continuum hydrodynamics. Multiscale Model. Sim. **3**, 749–763 (2005).
[31] Qian, T., Wang, X. P., Sheng, P.: Generalized Navier boundary condition for the moving contact line. Commun. Math. Sci. **1**, 333–341 (2003).
[32] Qian, T., Wang, X. P., Sheng, P.: Molecular scale contact line hydrodynamics of immiscible flows. Phys. Rev. E. **68**, 016306 (2003).

[33] Qian, T., Wang, X. P., Sheng, P.: Power-law slip profile of the moving contact line in two-phase immiscible flows. Phys. Rev. Lett. **93**, 094501 (2004).
[34] Qian, T., Wang, X. P., Sheng, P.: Hydrodynamic slip boundary condition at chemically patterned surfaces: a continuum deduction from molecular dynamics. Phys. Rev. E. **72**, 022501 (2005).
[35] Thompson, P. A., Troian, S. M.: A general boundary condition for liquid flow at solid surfaces. Nature **389**, 360–362 (1997).
[36] Happel, J., Brenner, H.: Low Reynolds number hydrodynamics. Prentice-Hall 1965.

Authors' address: M. T. Matthews and J. M. Hill, Nanomechanics Group, School of Mathematics and Applied Statistics, University of Wollongong, Wollongong 2522, N.S.W., Australia (E-mail: miccal@uow.edu.au)